Volume 17, Number 3, 2024. pp. 261-271

Jordan Journal of Physics

ARTICLE

Time Dependent Spectral Ratio Technique for Micro-seismic Exploration in the Niger Delta Region of Nigeria

Emetere Moses Eterigho[a,b]

[a] *Department of Physics, Bowen University Iwo, Nigeria.*

[b] *Department of Mechanical Engineering Science, University of Johannesburg, South Africa.*

Doi: **https://doi.org/10.47011/17.3.1**

Received on: 05/01/2022; *Accepted on: 12/12/2022*

Abstract: Since the discovery of the hydrocarbon micro-tremors, there have been numerous efforts to understand the causes of these microseisms related to oil and gas. A spectral ratio (SR) time-dependent equation was derived based on geological principles. The equation showed tremendous success in analyzing multi-layered geological terrain and estimating the spectral ratio in the Niger Delta region of Nigeria. This study seeks to develop a reliable model using standard seismic reflection data to analyze microseismic datasets from hydrocarbon reservoirs. Type A-SR acts over a longer duration and can be used to determine hydrocarbon reservoirs. Type B-SR acts in a short time with maximum impact. It can be used to determine gas condensate flow in the hydrocarbon reservoir. It is recommended that this technique be applied in real time to ascertain its accuracy.

Keywords: Niger Delta, Microseismic, Amplitude, Special ratio, Geology.

Introduction

The outcomes of seismic investigations have increasingly become complex due to puzzling geological features within the subsurface and depositional trends [1]. Advances in new technologies and numerically efficient computing systems have provided an in-depth understanding of subsurface complexity [2]. However, a few anomalies in understanding the subsurface may stem from the foundational theories of the equipment or technique used. So far, numerical solutions of mathematically derived seismic attributes are salient in pre-modeling complex situations. Thus, this concept is a critical part of the model-building technique for the determination of seismic imaging and attribute anomalies.

The horizontal-to-vertical (H/V) spectral ratio of the seismic noise technique has gained wide usage since it was proposed by Nogoshi and Igarashi [3, 4]. This technique has proven to be very useful in a deltaic environment for characterizing the sediments on top of the bedrock [5-7]. The technique basically computes the ratio between the Fourier amplitude spectra of the horizontal and vertical components of seismic noise measurements, as depicted in the formula below:

$$\frac{H}{V} = \frac{S_{NS}+S_{EW}}{2*S_V} \quad (1)$$

where S_{NS}, S_{EW}, and S_V are the magnitudes of the smoothed Fourier spectra of the north-south, east-west, and vertical components, respectively. The experimental factors often affect the H/V spectral ratio (HVSR) results. These factors include complex geological terrains, subsalts, formations beneath volcanic rocks, formations with low acoustic impedance contrast, and seismic damage distributions [8, 9]. Also, the general trends of the H/V technique indicate that horizontal motion is larger than vertical motion on soft ground, while horizontal and vertical motions are similar on hard ground. This can

Corresponding Author: Emetere Moses E. **Email**: emeteremoses@gmail.com

pose a major challenge when the geology terrain includes integrated profiles of hard and soft ground or rock formations.

Basically, the HVSR is mainly obtained from microtremor surveys. Beyond its above-listed application, the HVSR technique is now adopted in oil and gas exploration for estimating drilling risk and monitoring reservoirs [10, 11]. Haris *et al.* compared the results of microtremor surveys and time-reverse modeling (TRM) over a hydrocarbon reservoir [12]. It was observed that HVSR showed a potential hydrocarbon zone, while TRM predicted the depth range of this zone. HVSR is used for modeling sedimentary basins using a simple two-layer model, consisting of node side (hard rock basement) and open-end (surface of the basin).

Hydrocarbon reservoirs within the sedimentary basin act as frequency converters, producing a unique spectral signature that is used as a direct hydrocarbon indicator. Many companies have affirmed that low-frequency passive seismic anomalies are common features of hydrocarbon reservoirs [13, 14].

However, the quality of signal resolution is quite important as it helps clarify the effects of some geological features. Q estimation is widely used, as it is a proven tool to obtain better signal resolution via inverse Q filtering principles. Q refers to the attenuation factor of the transmitted seismic wavelet. Various scientists who have worked on the building technique of seismic technologies have made discoveries that show the dynamism of the subsurface. For example, the cyclic succession of sand and shale properties was used to create a 1D seismic model for lithological elements [15]. The Q estimation factor for quantifying attenuation has been used to characterize rock properties, reservoir heterogeneity, and subtle geological structures [14, 16, 17]. Q can also be used in reservoir characterization [17].

It has been established that the zero-offset ray-tracing technique for primary P waves is efficient for creating a 2D seismic model to predict the seismic responses of geological features [18]. Therefore, Q-factor can be derived from transmission data, such as vertical seismic profiling (VSP) data [19], crosswell dataset [20], and sonic logging datasets [21]. Q estimation depends on frequency shifts in the geological or geotechnical setting. Li *et al.* [17] used this concept (frequency shifting) to prevent the exponential decay of seismic amplitude with respect to time and depth. In other words, Q estimation is largely dependent on theoretical configurations. These configurations include time-domain modification of the spectral ratio method [22], statistical analysis of spectral ratio [23], frequency shift method [17], and spectral ratio time-dependent method [24], all of which are essential for fieldwork to obtain Q-factor.

Since the discovery of hydrocarbon microtremors, there have been numerous efforts to understand the causes of this phenomenon related to oil and gas [25]. In this paper, the time-dependent spectral ratio (TDSR) is modified to enable the use of standard seismic reflection data to analyze the microseismic emissions from hydrocarbon reservoirs. The second section of the paper introduces the theoretical formulations. The mathematical implications of the technicalities of the theory are explained in the third section. The application of the new theory to an oil field is illustrated in the fourth section. The oil field is located in the Niger Delta region of Nigeria. The surface geology of the region is illustrated in the red box in Fig. 1.

Background Theories and Formulation

Seismic waves lose energy and magnitude of frequency when traveling through the subsurface of the Earth. The time-frequency decomposition $S(\tau,\omega)$ of a seismic trace $s(t)$ in the presence of inelastic attenuation Q and time-varying amplitude is given as:

$$S(\tau,\omega) = W(\omega) \times A(\tau) \times A_o exp\left(\frac{-\omega\tau}{2Q(\tau)}\right) \quad (2)$$

where ω is the frequency, τ is the time, $W(\omega)$ represents the frequency/amplitude spectrum of the underlying wavelet, $A(\tau)$ is the time-varying amplitude effect, and $A_o exp\left(\frac{-\omega\tau}{2Q(\tau)}\right)$ defines the time-varying Q contribution. Most researchers have tried to modify the amplitude using a constant Q model:

$$A_n(f) = A_o(f)\exp(-\frac{\pi f t}{Q}) \quad (3)$$

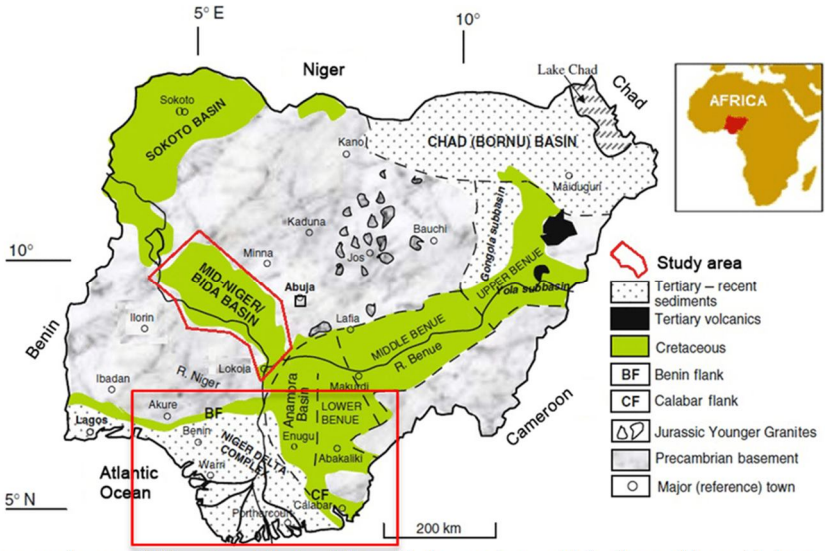

FIG. 1. Surface geology of Nigeria with the Niger Delta region within the red box (Adapted from [36]).

Emetere *et al*. modified the ratio of the amplitude in Eq. (3) and used Maclaurin's series to simulate the multilayer implementation of seismic signals through the subsurface [24]. From the amplitude misfit function and its corresponding gradient, the volume of hydrocarbons can be estimated using a multi-layer probe.

$$V_n = A\varphi.\frac{sQ}{\pi ft}\sum_{n=1}^{\infty}\sqrt[n]{\frac{A_n(f,t)}{A_o(f,t)}} \tag{4}$$

where A is the area of the areal extent of the deposition, s is the speed of the seismic probe, and φ is the porosity.

In this research, the time-frequency decomposition of two geographical points within the same location was adopted to modify Eq. (2). The mathematical implication is illustrated in Eq. (5). Technically, the reason for adopting two seismic signals is to capture the conversion processes as microseismic events come from passive seismology, while seismic reflection-wave surveys are related to active methods of seismic exploration [26].

$$S(\tau,\omega) = W(\omega_n-\omega_1)\times A(\tau_n-\tau_1)\times A_o exp\left(\frac{-(\omega_n-\omega_1)(\tau_n-\tau_1)}{2Q((\tau_n-\tau_1))}\right) \tag{5}$$

where $W(\omega) = \sin(2n\pi\omega\tau) + \cos(2n\pi\omega\tau)$

Hence, adopting the assumption that $\omega_n\tau_1 = 0\ and\ \omega_1\tau_n = 0$, the expanded Eq. (5) becomes:

$$S(\tau,\omega) = \{\sin(2n\pi\omega_1\tau_1(\cos(2n\pi\omega_n\tau_n) - \sin(2n\pi\omega_n\tau_n)) + \cos(2n\pi\omega_1\tau_1(\sin(2n\pi\omega_n\tau_n) + \cos(2n\pi\omega_n\tau_n))\}\times A(\Delta\tau)\times A_o exp\left(\frac{\omega_1\tau_1-\omega_n\tau_n}{2Q(\Delta\tau)}\right) \tag{6}$$

Dividing Eq. (6) by Eq. (5) under the assumption that $Q(\tau)\approx Q(\Delta\tau)$, we get:

$$\frac{A(\Delta\tau)}{A(\tau)} = \frac{\sin(2n\pi\omega\tau)+\cos(2n\pi\omega\tau)}{\sin(2n\pi\omega_1\tau_1(\cos(2n\pi\omega_n\tau_n)-\sin(2n\pi\omega_n\tau_n))+\cos(2n\pi\omega_1\tau_1(\sin(2n\pi\omega_n\tau_n)+\cos(2n\pi\omega_n\tau_n))}\times exp\left(\frac{\omega_1\tau_1}{2Q(\tau)}\right) \tag{7}$$

or

$$\frac{A(\Delta\tau)}{A(\tau)} = \frac{\sin(2n\pi\omega\tau)+\cos(2n\pi\omega\tau)}{\sin(2n\pi\omega_1\tau_1(\cos(2n\pi\omega_n\tau_n)-\sin(2n\pi\omega_n\tau_n))+\cos(2n\pi\omega_1\tau_1(\sin(2n\pi\omega_n\tau_n)+\cos(2n\pi\omega_n\tau_n))}\times exp\left(\frac{-2\omega_1\tau_1+\omega_n\tau_n}{2Q(\tau)}\right) \tag{8}$$

However, based on the estimation of individual seismic signals at each geographical point, Eqs. (7) and (8) can be simplified into :

$$\frac{A(\Delta\tau)}{A(\tau)} = \frac{\sin(2n\pi\omega_n\tau_n)+\cos(2n\pi\omega_n\tau_n)}{\sin(2n\pi\omega_1\tau_1(\cos(2n\pi\omega_n\tau_n)-\sin(2n\pi\omega_n\tau_n))+\cos(2n\pi\omega_1\tau_1(\sin(2n\pi\omega_n\tau_n)+\cos(2n\pi\omega_n\tau_n))}\times exp\left(\frac{\omega_1\tau_1}{2Q(\tau)}\right) \tag{9}$$

or

$$\frac{A(\Delta\tau)}{A(\tau)} = \frac{\sin(2n\pi\omega_n\tau_n)+\cos(2n\pi\omega_n\tau_n)}{\sin(2n\pi\omega_1\tau_1(\cos(2n\pi\omega_n\tau_n)-\sin(2n\pi\omega_n\tau_n))} \times \\ +\cos(2n\pi\omega_1\tau_1(\sin(2n\pi\omega_n\tau_n)+\cos(2n\pi\omega_n\tau_n)) \\ exp\left(\frac{-2\omega_1\tau_1+\omega_n\tau_n}{2Q(\tau)}\right) \quad (10)$$

$$\frac{A(\Delta\tau)}{A(\tau)} = \frac{\sin(2n\pi\omega_1\tau_1)+\cos(2n\pi\omega_1\tau_1)}{\sin(2n\pi\omega_1\tau_1(\cos(2n\pi\omega_n\tau_n)-\sin(2n\pi\omega_n\tau_n))} \times \\ +\cos(2n\pi\omega_1\tau_1(\sin(2n\pi\omega_n\tau_n)+\cos(2n\pi\omega_n\tau_n)) \\ exp\left(\frac{\omega_1\tau_1}{2Q(\tau)}\right) \quad (11)$$

or

$$\frac{A(\Delta\tau)}{A(\tau)} = \frac{\sin(2n\pi\omega_1\tau_1)+\cos(2n\pi\omega_1\tau_1)}{\sin(2n\pi\omega_1\tau_1(\cos(2n\pi\omega_n\tau_n)-\sin(2n\pi\omega_n\tau_n))} \times \\ +\cos(2n\pi\omega_1\tau_1(\sin(2n\pi\omega_n\tau_n)+\cos(2n\pi\omega_n\tau_n)) \\ exp\left(\frac{-2\omega_1\tau_1+\omega_n\tau_n}{2Q(\tau)}\right) \quad (12)$$

Numerical Analysis of the Spectral Amplitude on the Niger Delta Field

The parameters adopted in this section were obtained from Barton, where the Q factor ranged between 26 and 200 and the frequency between 450 and 725 Hz [27]. Though the travel time of S waves through the sedimentary rock was estimated by Campbell to be 1.10 s [28], a maximum time of 4 s was considered to accommodate the physics of the site attenuation (Q) parameter, which may dependend on either the maximum frequency [29, 30] or corner frequency. The spectral amplitude was observed to gradually decrease with depth in the inhomogeneous subsurface. The decrease trend of the SR method with respect to time was monitored as shown in Figs. 2-4.

Figure 2(a) presents a scenario where $A_n(f,t)$ and $A_o(f,t)$ are in their original forms. The amplitude misfit is highest at the maximum spectral and modified amplitudes. The projections of the spectral and modified amplitudes are shown in Figs. 2(b) and 2(c). These features suggest that the trends of the spectral and modified amplitudes are critical for understanding deposits incomplex geological settings like the Niger Delta. This is because the distribution of sub-weathering velocities in the subsurface is affected by high-velocity Palaeozoic carbonates and lower-velocity Cretaceous clastic [31]. When a multi-layered petroleum system is considered in the complex geometry, as described by Eq. (4), the distribution of sub-weathering velocities changes, as shown in Figs. 3-4. Figures 3(a) and 4(a) depict the sine and cosine forms of the amplitude misfit under the influence of the individual spectral and modified amplitudes.

Application of Spectral Amplitude: Case Study of the Niger Delta Field

The cross-sectional profile of the Akata Formation in the Niger Delta region of Nigeria is presented in Fig. 5.

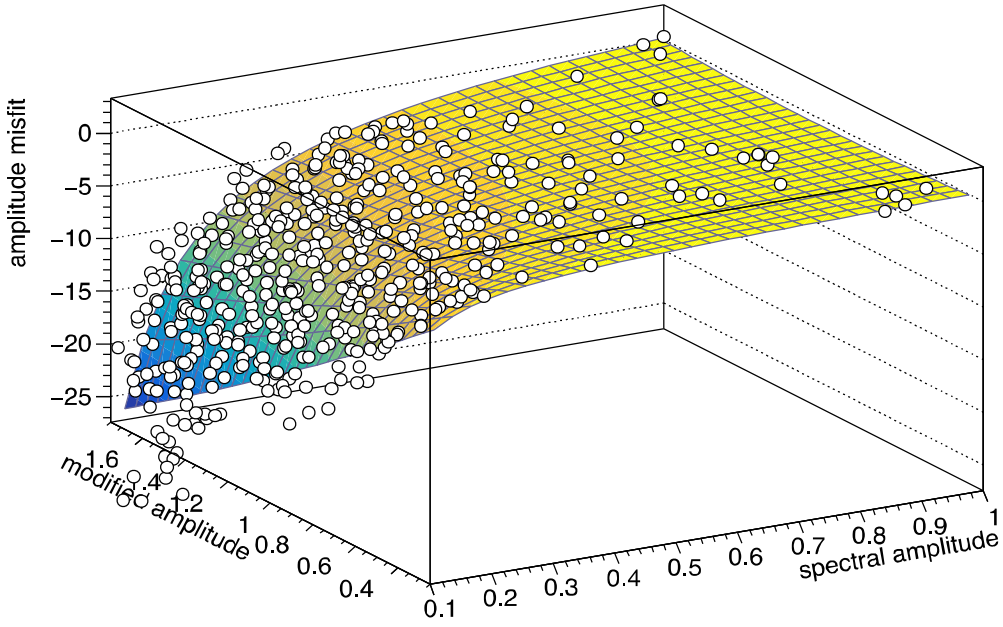

FIG. 2(a). $A_n(f,t)$ and $A_o(f,t)$ in their original form.

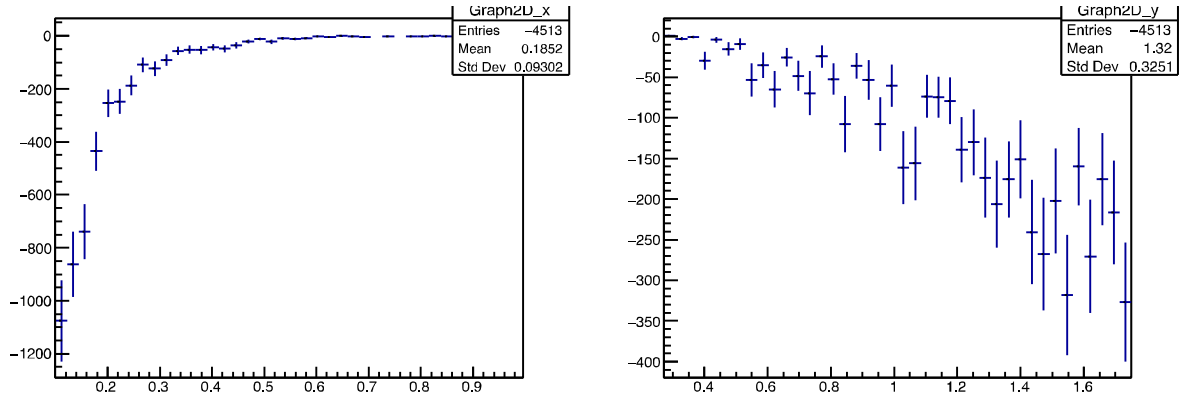

FIG. 2. (b) The misfit amplitude projection under the influence of $A_o(f,t)$. (c) The misfit amplitude projection under the influence of $A_n(f,t)$.

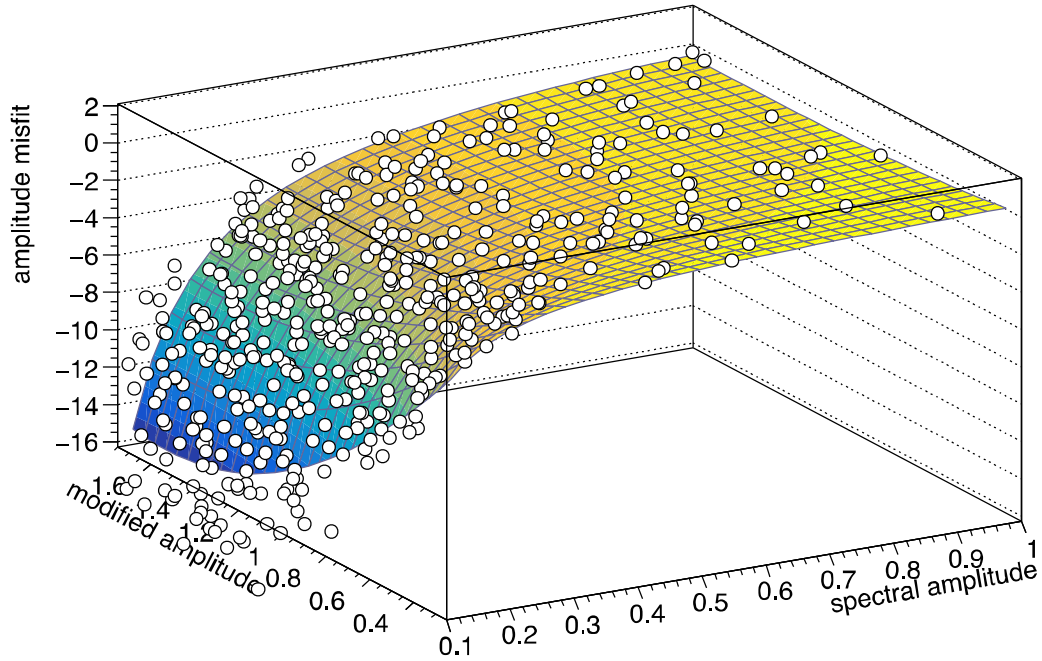

FIG. 3(a). $A_n(f,t)$ and $A_o(f,t)$ in their sine form.

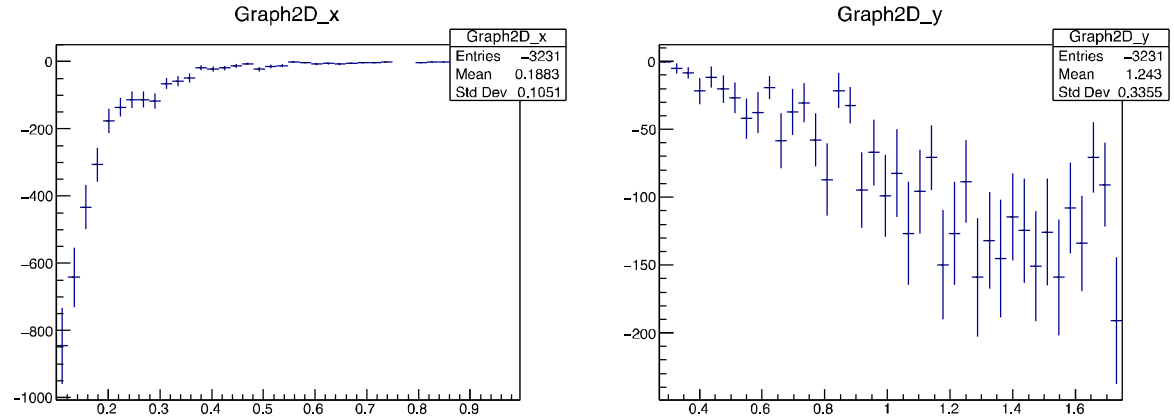

FIG. 3. (b) The misfit amplitude projection under the influence of the sine form of $A_o(f,t)$. (c) The misfit amplitude projection under the influence of the sine form of $A_n(f,t)$.

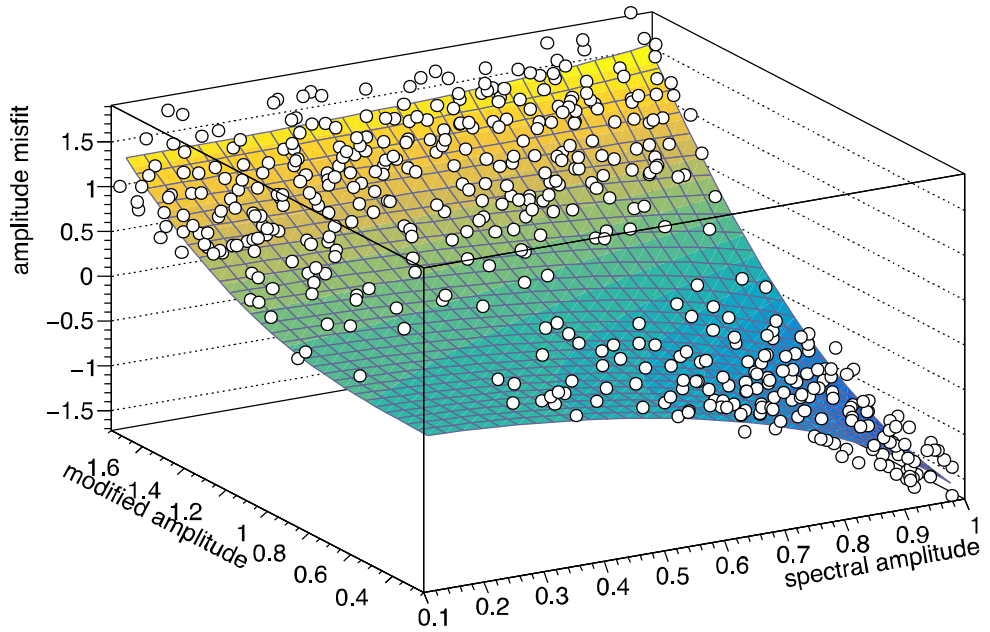

FIG. 4(a). $A_n(f,t)$ and $A_o(f,t)$ in their cosine form.

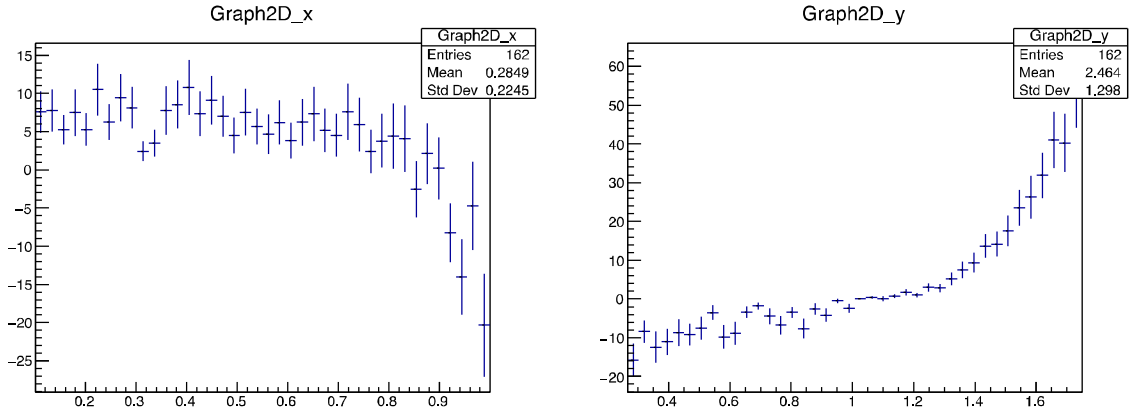

FIG. 4. (b) The misfit amplitude projection under the influence of the cosine form of $A_o(f,t)$. (c) The misfit amplitude projection under the influence of the cosine form of $A_n(f,t)$.

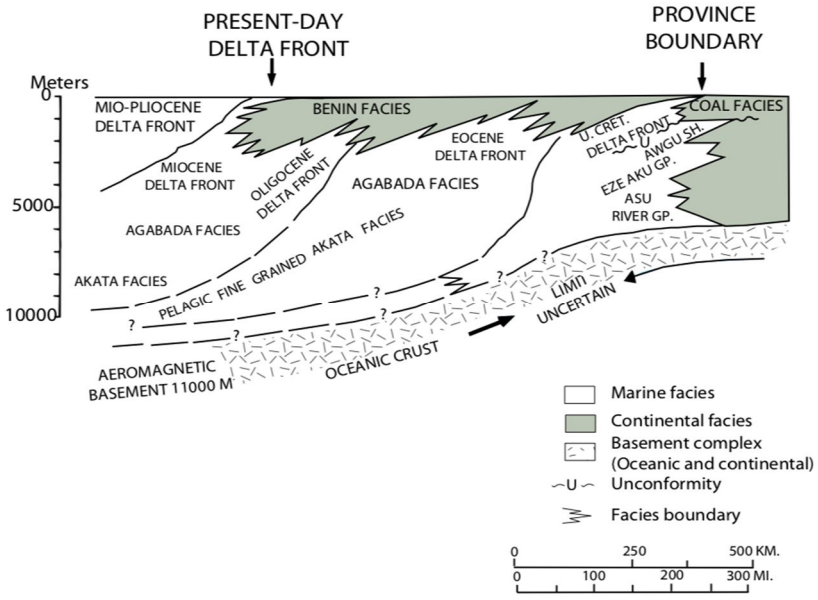

FIG. 5. The depth profile of the Niger Delta region [32].

The Akata Formation is known to have the highest number of hydrocarbon reservoirs in the Niger Delta [33-35]. The primary source rocks in the Niger Delta petroleum system include the upper Akata Formation, the marine-shale facies of the delta, and the interbedded marine shale of the lowermost Agbada Formation. The higher-density delta-front sands in the Agbada Formation and the under-compacted delta-slope clays in the Akata Formation influence seismic transmission in the Niger Delta as presented in Fig. 5 [32].

In this study, the depth profile analysis of the Akata Formation is illustrated in Fig. 6. Two seismic signals are presented in Fig. 6. The source of the dataset is documented in Tuttle *et al*. [32]. The iso-reflectance (Ro) values and their corresponding depths are 0.6 at 2.5 km, 0.8 at 3.2 km, 1.2 at 4.2 km, and 2.0 at 5.4 km.

The theory presented in Eqs. (2)-(12) propounds that two seismic signals within the same geographical site can generate microseismic events, which are used to determine salient geological features, such as hydrocarbon reservoirs. The two seismic signals presented in Fig. 6 are analyzed at two different depths: 6 km and 7 km. The combined effect of the two seismic signals depends on the reference frame chosen. If the higher seismic signal is used as the reference, Eq. (7) applies. Similarly, if the lower seismic signal is the reference, Eq. (8) is applied. Furthermore, Eqs. (7) and (8) can be classified into individual seismic signals, as presented in Eqs. (9)-(12). Equation (12) is referred to as case 1, Eq. (10) as case 2, Eq. (11) as case 3, and Eq. (9) as case 4.

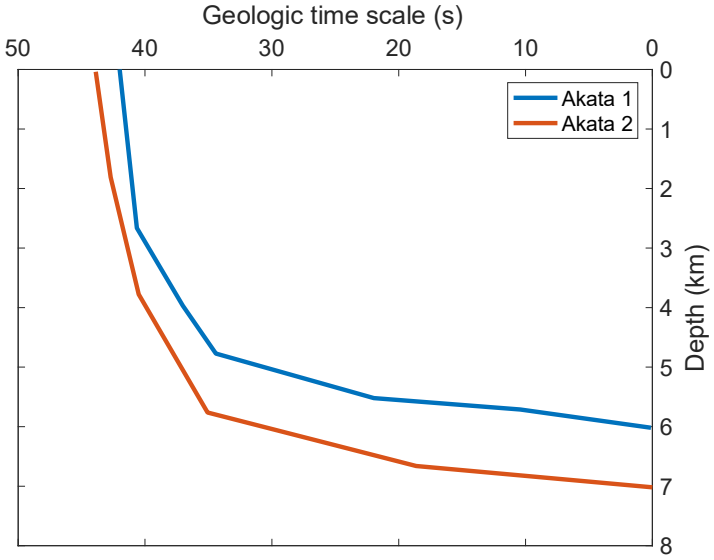

FIG. 6. Depth profile of two close seismic signals in Akata Formation.

The spectral ratio against the depth for $exp\left(\frac{-2\omega_1\tau_1+\omega_n\tau_n}{2Q(\tau)}\right)$ is presented in Fig. 7. This scenario reflects a situation where the lower seismic signal dominates the microseismic events. Usually, the microtremors of hydrocarbons have energy in the low-frequency spectrum. Hence, there is a possibility of wave superposition if an experiment is carried out in real time. In this case, it was observed that the hydrocarbon microtremor (HDM) could be found within 6-7 km depth in the Niger Delta region. This spectral ratio, termed Type A-SR, is generally lower compared to scenarios where higher seismic signals dominate, as presented in Fig. 8.

The advantage of the latter scenario, where a larger seismic signal dominates the micro-seismic event, is its potential to locate the gas condensate flows, found at the depth of 1850 m in this study. It is salient to note that the above condition leads to spectral ratio attenuation to zero at lower depths (Fig. 8). This type of spectral ratio is named Type B-SR. The hypothesis in this regard is that there will be spectral ratio quenching at higher depths when the seismic signal is $exp\left(\frac{\omega_1\tau_1}{2Q(\tau)}\right)$.

The analysis of the spectral ratio versus the geological time scale is presented in Figs. 9 and 10. Type A-SR has a broad operational duration with its maximum at 18 s (Fig. 9). Hence, the HDM can also be estimated at a maximum (type A) spectral ratio when the exponential conversion from the seismic reflection wave

survey to the micro-seismic event is $\left(\frac{-2\omega_1\tau_1+\omega_n\tau_n}{2Q(\tau)}\right)$. Also, it was observed that the Type B-SR acts within a short time at high magnitude (Fig. 10) when the exponential conversion from the seismic reflection wave survey to the micro-seismic event is $\left(\frac{\omega_1\tau_1}{2Q(\tau)}\right)$.

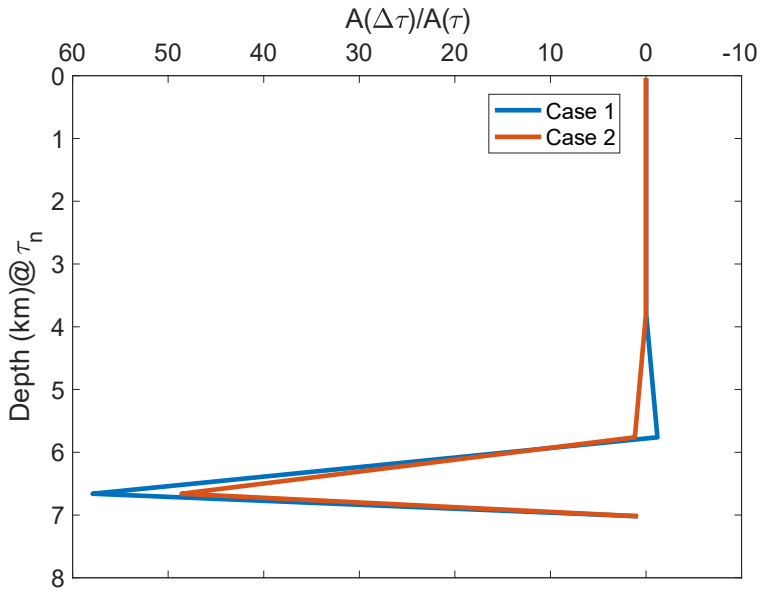

FIG. 7. Spectral ratio variation within $exp\left(\frac{-2\omega_1\tau_1+\omega_n\tau_n}{2Q(\tau)}\right)$ depth profile.

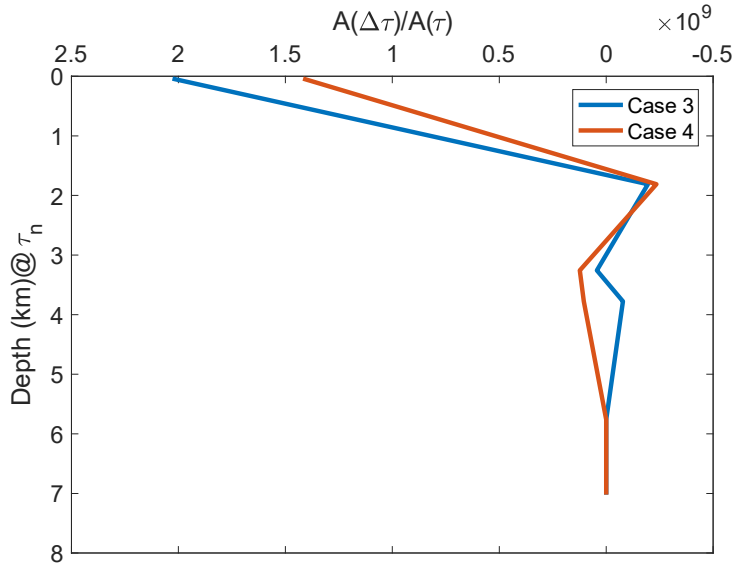

FIG. 8. Spectral ratio variation within $exp\left(\frac{\omega_1\tau_1}{2Q(\tau)}\right)$ depth profile.

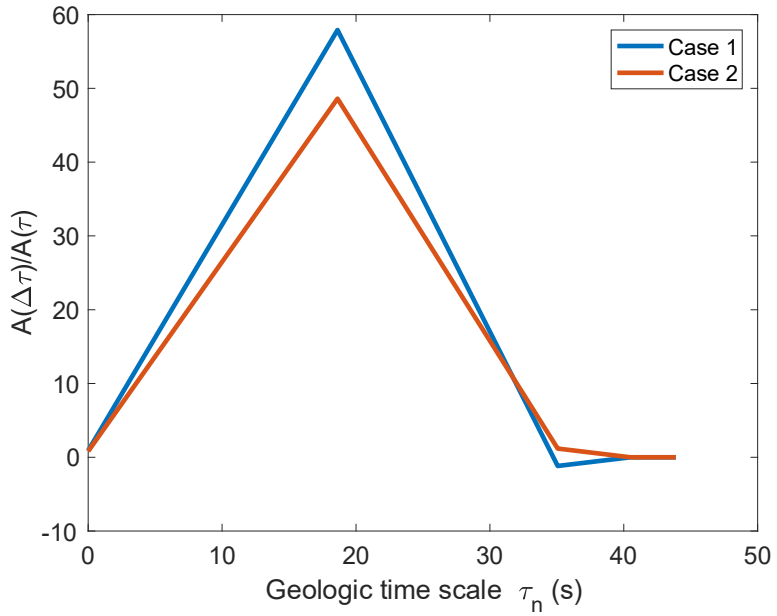

FIG. 9. Spectral ratio variation within $exp\left(\frac{-2\omega_1\tau_1+\omega_n\tau_n}{2Q(\tau)}\right)$ geologic time scale.

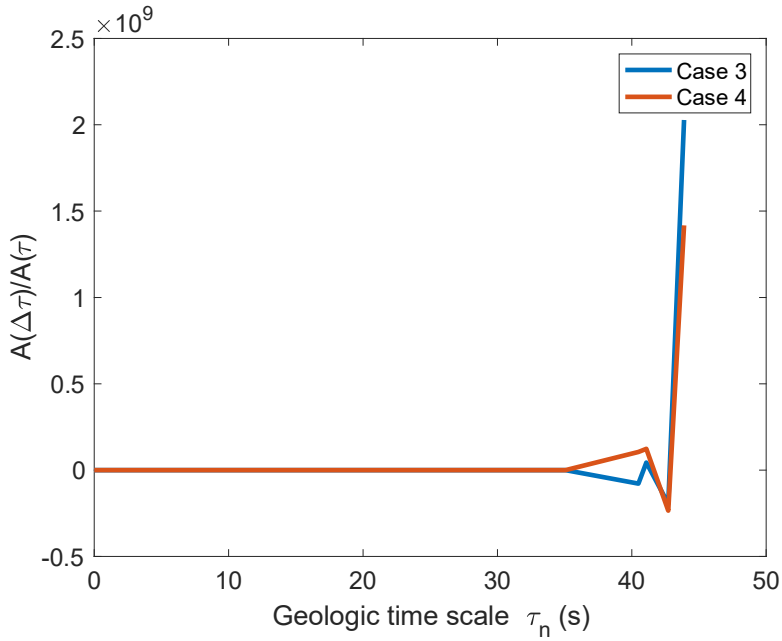

FIG. 10. Spectral ratio variation within $exp\left(\frac{\omega_1\tau_1}{2Q(\tau)}\right)$ geologic time scale.

In other words, the actual determination of the HDM depends on the seismic signal and the geological profiles of a geographical location.

Conclusion

These features of the SR time-dependent method suggest that the trend of the spectral and modified amplitudes is a vital parameter for understanding deposits within the complex geology of a petroleum system. The distribution of sub-weathering velocities in the subsurface is determined by the magnitude of the spectral and modified amplitudes. The adoption of the SR time-dependent method in a complex geological setting, such as the Niger Delta, depends on the active to passive seismic conversion process between two seismic signals within the same geographical location. Two types of spectral ratios were proposed. Type A spectral ratio acts over a longer time and can be used to determine hydrocarbon reservoirs. Type B spectral ratio acts over a shorter time with maximum impact and can be used to detect gas condensate flow in the hydrocarbon reservoir. It is recommended that this technique be applied in real time to ascertain its accuracy.

Conflict of interest

The author declares no competitive interest.

Data Availability Statement

Some or all data, models, or codes that support the findings of this study are available from the corresponding author upon reasonable request.

References

[1] Piazza, J.L., Donati, M., Martin, F.D., Castro, J., Gordillo, C., and Belhouchet, T., 76th EAGE Conference and Exhibition, Amsterdam, (2014).

[2] Alaei, B. and Petersen, S.A., Pet. Geosci., 13 (2007) 241.

[3] Nogoshi, M. and Igarashi, T., J. Seism. Soc. Japan, 23 (1970) 264.

[4] Nogoshi, M. and Igarashi, T., J. Seism. Soc. Japan, 24 (1971) 26.

[5] Xu, R. and Wang, L., EURASIP J. Adv. Signal Process, 2021 (2021) 75.

[6] Bonnefoy-Claudet, S., Baize, S., Bonilla, L.F., Berge-Thierry, C., Pasten, C., Campos, J., Volant, P., and Verdugo, R., Geophys. J. Int., 176 (2009) 925.

[7] Fah, D., Kinf, F., and Giardini, D., Geophys. J. Int., 145 (2001) 535.

[8] Farfour, M. and Yoon, W.J., J. Adv. Res., 7 (3) (2016) 515.

[9] Panou, A.A., Theodulidis, N.P., Hatzidimitriou, P.M., Stylianidis, K., and Papazachos, C.B., Soil Dyn. Earthq. Eng., 25 (2005) 261.

[10] Schmalholz, S.M., Podladchikov, Y.Y., Holzner, R., and Saenger, E.H., First EAGE Passive Seismic Workshop-Exploration and Monitoring Applications. European Association of Geoscientists and Engineers, Houten, Netherlands, (2006) p. A06.

[11] Saenger, E.H., Schmalholz, S.M., Podladchikov, Y.Y., Holzner, R., Lambert, M., Steiner, B., and Frehner, M., 69th EAGE Conference and Exhibition Incorporating SPE EUROPEC 2007. European Association of Geoscientists and Engineers, Houten, Netherlands, (2007) p. A033.

[12] Haris, A., Riyanto, A., Syahputra, R., Gunawan, A., Panguriseng, M.J., Nuratmaja, S., and Adriansyah, J. Geophys. Eng., 16 (2019) 16.

[13] Roy, B.N., Agarwal, S., Roy, K., and Rastogi, B.K., Biennial International Conference and Exposition on Petroleum Geophysics, (2012) p. 279.

[14] Korneev, V.A., Goloshubin, G.M., Daley, T.M., and Silin, D.B., Geophysics, 69 (2004) 522.

[15] Khattri, K. and Gir, R., Geophys. Prospect., 24 (1976) 454.

[16] Parra, J.O. and Hackert, C.L., The Leading Edge, 21 (2002) 564.

[17] Li, F., Zhou, H., Jiang, N., Bi, J., and Marfurt, K.J., J. Geophys. Eng., 12 (2015) 577.

[18] May, B., and Hron, F., Geophysics, 43(6) (1978) 1119

[19] Tonn, R., Geophys. Prosp., 39 (1991) 1.

[20] Quan, Y. and Harris, J.M., Geophysics, 62 (1997) 895.

[21] Sun, X., Tang, X., Cheng, C.H., and Frazer, L.N., Geophysics, 65 (2000) 755.

[22] Cheng, P. and Margrave, G.F., 82nd Annual International Meeting, SEG, Expanded Abstracts, (2012) 1.

[23] Sun, S.Z., Wang, Y., Sun, X., Yue, H., Yang, W., and Li, C., 84th Annual International Meeting, SEG, Expanded Abstracts, (2014) 3709.

[24] Emetere, M.E., Oritseneyemi, C.T., and Ojo, O.O., Pet. Coal, 59 (3) (2015) 319.

[25] Holzner, R., Eschle, P., Dangel, S., Frehner, M., Narayanan, C., and Lakehal, D., Commun. Nonlinear Sci. Numer. Simul., 14 (2009) 160.

[26] Chichinina, T.I., Hogoev, E.A., and Reyes-Pimentel, A., 76th EAGE Conference and Exhibition, Amsterdam, Netherlands, (2014), 1.

[27] Barton, N., "Rock Quality, Seismic Velocity, Attenuation and Anisotropy", (Taylor and Francis, London, 2006).

[28] Campbell, K.W., Bull. Seismol. Soc. Am., 99 (4) (2009) 2365.

[29] Hanks, T.C., Bull. Seismol. Soc. Am., 72 (1982) 1867.

[30] Papageorgiou, A.S. and Aki, K., Bull. Seismol. Soc. Am., 73 (1983) 953.

[31] Helen, I. and Don, L., AAPG Annual Convention, Denver, Colorado, June 7-10, (2009).

[32] Tuttle, L.W., Mlchele, R.R.C., and Michael, E.B., USGS Open-File Report 99-50-H, (1999).

[33] Aigbedion, I. and Aigbedion, H.O., Int. J. Geosci., 2 (2011) 179.

[34] Ihianle, O.E., Alile, O.M., Azi, S.O., Airen, J.O., and Osuji, O.U., Sci. Technol., 3 (2) (2013) 47.

[35] Ameloko, A.A. and Owoseni, A.M., Int. J Innov. Sci. Res., 15 (2015) 193.

[36] Obaje, N.G. et al., "Geology and mineral resources of Nigeria". Lecture Notes in Earth Sciences, (2009).